Guruswamy, S. and M.E. Wadsworth. *Metallurgical Aspects in Cold Fusion Experiments*. in *The First Annual Conference on Cold Fusion*. 1990. University of Utah Research Park, Salt Lake City, Utah: National Cold Fusion Institute.

METALLURGICAL ASPECTS IN COLD FUSION EXPERIMENTS

SIVARAMAN GURUSWAMY and MILTON E. WADSWORTH
National Cold Fusion Institute, University of Utah

ABSTRACT

Deuterium loading of palladium cathodes in Pons-Fleischmann type electrolytic cells has been observed to result in generation of excess heat on several occasions. Metallurgical examination of some of the electrodes showed extensive damage associated with deuterium loading. Surfaces have been found to be covered with large number of impurities. Initiation and sustaining these heat bursts, monitoring of nuclear products and materials aspects of these electrolytic cells have been the focus of our current efforts. As D/Pd loading appear to be critical, the measurement of deuterium loading using dilatometry as a function of current density, surface and heat treatment of the cathode and poisoning are currently being investigated.

INTRODUCTION

High hydrogen gas fugacities or gas pressures at the cathode surfaces during aqueous electrolysis is not new to electrochemists or metallurgists, but the idea of Pons and Fleischmann [1] that such electro-chemically imposed pressures can be utilised to create conditions for fusion in the metal lattice was revolutionary. This appealing concept and the apparent simplicity of the experiment, resulted in the feverish international activity to replicate and as well as to provide explanations for their observations. Despite many negative claims, a significant number of laboratories report excess heat either at low continuous level or large short duration heat bursts [1-11], tritium at levels as high as 10^6 times the background [2,6,7,12,13], neutron bursts at levels of 10^{-8} times tritium level [6,7,12] and 3 MeV proton emissions [14] in electrolytic cells. These provide signals that nuclear processes may be occurring in these deuterated metals as suggested by Pons and Fleischmann. However there has been no consistent pattern in observations and the reproducibilty of experiments have been very poor. These may be attributed to the large number of metallurgical and electrochemical variables involved in these experiments as listed in Table 1.

Excited by the prospects of cold fusion and the key role metallurgists may play in this technology, an experimental program was initiated to determine metallurgical changes, structural integrity of the electrodes and possible alternate metals and alloys. After several weeks of charging 4 mm diameter Pd cathodes with deuterium by electrolysis in 0.1 M LiOD solution at high overvoltages, modest to large heat releases were observed. The deuterated electrodes have been examined for changes in metallurgical structure and

surface chemistry. The extent of loading under typical electrolysis conditions has been determined using dilatometry and gravimetric techniques. Metallurgical factors influencing D/Pd loading, problems involved in measuring D/Pd ratio by various techniques are discussed. Current efforts are aimed at monitoring in-situ changes in the Pd electrode characteristics, electrochemical conditions, preparation of Pd electrodes with controlled impurities and additives to enable a better understanding of processes occuring in these cells.

CELL CONFIGURATION AND OPERATION

Different designs of large cells used in our study are shown in figures 1 a, b & c. Large 4 mm diameter × 10 cm long Pd rod cathodes and Pt windings or mesh or sheet supported by a glass rod cage anodes are used in these cells. Continuous heavy water addition to the cell is done using syringe pumps. The first cell design (Figure 1a) had one thermocouple to measure the cell temperature. To have redundancy in temperature measurement, three temperature sensors, one at the top, one at the middle and one at the bottom section of the cells, were used in the latter designs. Internal / external recombination of deuterium and oxygen from the electrolysis was done in most of our cells. The cells were operated mostly in a constant current mode. The cell operation is automated both in D_2O addition and data recording. Temperature, voltage, current and other signals are sampled every 10 seconds and recorded every 1 minute. When sudden changes in cell operating conditions were sensed, recording then occurs every 10 seconds. The temperatures inside the cell and the temperature of the bath in conjunction with calibration curves are used to measure the power output level. Bath temperature is maintained within 0.01°C. Thermal calibration is done by performing electrolysis at different power levels as well as by using an internal heater. Laser Doppler measurement of bubble velocities in the cell (Figure 1d) showed excellent stirring by the evolved gas bubbles resulting in very uniform temperature distribution, within 1°C over most regions of the cell. Flow patterns in the cell were studied by measuring velocities of the gas bubbles using a Laser. Lithium concentration, electrolyte conductivity and pH are monitored periodically. Li concentration is measured using DCP analysis. The cathode metals tested were palladium, titanium and zirconium. However most of the attention was focused on palladium. Platinum and nickel wire, gauze and sheets have been used as anodes. The experimental variables tested included the form of the platinum anode, anode to cathode surface area, anode to cathode distance, separation of deuterium and oxygen using a Nafion membrane that allows deuterium ion to pass through but not the anion, preloading of deuterium under high pressure deuterium gas, and variation in the heat and surface treatment of the palladium cathode.

TEMPERATURE EXCURSIONS SHOWING EXCESS POWER GENERATION

During the first week of May, 1989, frequent explosive popping of the cells (Figure 2a) were observed, some with minimal damage and some with the destruction of the assembly. The temperature excursions were associated with some of these events which were initially dismissed as being due to deuterium and oxygen recombination. Again in the third week of May, a large temperature excursion of about 12°C was observed, the cell temperature rise lasting about 90 minutes (Figure 2a). The temperature-time profiles

showed a similar pattern to an earlier temperature excursion (Figure 2b). This particular cell was operating at constant current mode at current setting of 0.95 amperes during the heat excursion shown in Figure 2a. The voltage was recorded continuously while the current was manually recorded. The temperature excursion was interrupted by the make up D_2O addition. During the burst shown in Figure 2b, the cell was being operated in a constant voltage mode and the voltage and current readings were manually recorded. Explosive popping of the cell interrupted the large heat burst and dislodged the electrodes. The cell was put back together immediately and the cell temperature remained at a level well above the normal values corresponding to the gross power input to the cell (about 9.6 Watts). Thermal calibration curves showed that excess heat generated during these two events were about 240,000 Joules during the 91 minute burst and around 1 MJ during the 40 minute burst followed by a 30 hour excess heat generation at a lower level. During the bursts the power outputs were as high as 6-7 times the input power which was less than 10 Watts. This level of energy output could not be explained by burning of all the deuterium stored in the Pd cathode, the heat of solution of deuterium in palladium, or the heat of formation of PdD_x. We also checked the possibility of storing energy in the solution in the form of peroxide. Analysis of electrolyte samples from all the operating cells showed peroxide concentration was less than 10^{-4} moles/cm^3 as expected from the instability of peroxide under high cathodic overvoltage conditions. The tritium level in the electrolyte after degassing of the electrode that showed the 90 minute heat burst and the starting solutions were checked by 3 different laboratories. The level of tritium was found to have increased by a factor of 3-4 which is more than can be accounted for by separation during electrolysis. The electrode (JM 2) involved in the above two large heat bursts was the same and had been obtained from Johnson Matthey and had a purity of 99.95%. The heat treatment involved annealing at 600°C in ultra high purity argon atmosphere. Figures 2c and 2d show two consecutive bursts in a same cell using a high purity Pd rod, (Electrode #5), from Metalor, USA. In all the above heat excursions cell design shown in figure 1a had been used. A single thermocouple was used to monitor the cell temperatures.

Figure 2e shows operating cell data for Cell 9 (Figure 1b). Each point corresponds to an average temperature and power input data for a period during which the cell was operated at a given current level. During a period when the cell was operated at a current level of 2.0 Amperes, the temperature of the cell was about 1.8°C (about 7.6 excess Watts) above the expected value suggesting excess power production during this period. No excess tritium was seen in this cell. On 11 different occasions, we have seen events which seem to have generated excess heat.

Our earlier cells were designed to use large cathodes to provide enough material for subsequent metallurgical characterisation and therefore limited to detect only large excess heats. But these cells had rapid thermal response times of about 90 seconds. Our recent cell design with an external acrylic jacket (Figure 1c) has a cell constant of about 0.5 W/°C and a nearly linear response. Excess power of the order of 200-300 mW can be detected in these new cells. The relaxation time is less than 10 minutes and the size of the electrode / maximum power input to the cells is lower.

METALLURGICAL EXAMINATION OF ELECTRODES THAT SHOWED HEAT BURSTS

BULK ANALYSIS

A single palladium electrode has shown heat bursts illustrated in Figures 2a and 2b. This electrode was degassed and the electrolyte was sent for tritium analysis. The electrode was cleaned with distilled water and dried. Resistance measurement by four probe technique showed a two fold increase in resistivity. The electrode was then examined by positron annihilation technique.

The Doppler line broadening of the electron-positron annihilation peak at 512 keV showed a 6% change in the Peak/Width ratio which is rather large indicative of a large increase in defect density. The surface hardness along the length was first measured using a Vickers indentor at 1 kg load. Soft and hard spots at adjacent locations were observed. This is likely to be due to subsurface cracks and to hardness measurements on a curved surface. Smaller lengths of the electrode were cut from the lower half of the electrode and hardness measurements were made on the cut section. The hardness values obtained were very uniform showing values of 102 ±5 VHN. The hardness value for this material before the cell exposure was 69 VHN.

While the above electrode JM2 did not show visual cracking, another electrode from the same batch showed after more than 11 months of operation showed a high density of visual cracks on the surface. A 99.995 purity Pd rod from a different source deuterated for nearly 11 months showed extensive visual damage as shown in Figure 3. The surface contains a high density of fine cracks. Hardness measurements on the cross section show wide variation from 110 VHN to 180 VHN due to extensive microcracking in the sample. The optical microscopy image of the cross section shows extensive cracking and surface relief associated with subsurface cracks. Extensive cracking was also observed in electrode 17 which is a 0.5 mm wire subjected to current densities from 1000 - 3000 mA/cm^2 over a period of about 3 months.

TRANSMISSION ELECTRON MICROSCOPY

Thin slices cut from electrode JM2 were mechanically polished and then electro-chemically thinned for observation of the internal structure. The diffraction pattern confirmed the presence of β hydride phase which is a metastable phase. The electrode after the cell operation, showed extensive deformation and much larger dislocation density compared to the annealed starting material as can be seen from Figures 4 a & b. The damage observed may be due to large strain associated with β hydride phase formation and/or the deformation resulting from high pressure hydrogen bubbles. In the future it will be very important to make a comparison of the internal damage for identical rods, one of which has experienced excess heat generation.

Figure 4c shows a TEM micrograph of electrode 5 after about 11 months of electrolysis. Specimen preparation of this sample was particularly difficult and image is less clear due to extensive strain, high dislocation density and micro-cracks.

X-RAY DIFFRACTION

An X-ray diffraction pattern showed that the major phase was β hydride. Only minor amounts of α phase were observed. The D/Pd ratio in the sample was estimated to be around 0.7.

SURFACE ANALYSIS

Surface chemical analysis was done using different techniques. A quick examination of the near surface region was performed using the state of the art CAMECA 50 SX electron microprobe. This showed only palladium with trace amounts of Rh and Br. Possible rhodium contamination from the platinum anode is possible. Sampling volume in this technique is 1 μm^3 and light elements below carbon and trace elements may not be detected by this technique. XPS, Auger electron spectroscopy and SIMS analysis were performed at the Battelle Nothwest laboratories. Perkin-Elmer Physical Electronics 550 multiprobe surface analysis system was used. AES analysis was done using 5 kV electron beam. XPS data was generated using Mg K_α X-rays. The SIMS analysis was performed using a 5 KV Ar ion beam to detect trace impurities. The quantitative estimates of different elements present in the first few nanometers of the surface region using XPS and Auger analysis are shown in Tables 2 and 3. Both XPS and AES data shows that the surface is highly contaminated with O and C contaminants that come from handling. Other minor contaminants are expected, except probably Co, from the electrolyte, anode, quartz glass vessel or from handling. SIMS profile over a depth of about 600 nm is shown in Figure 5 (sputtering rate of about 6 nm/mt) and Li signal amplitudes at different depths ratioed to Pd signal are summarised in Table 4. High surface enrichment of Li and a surprisingly very small amount of Pd. Surface is covered with elements such as Al^{27}, Na^{23}, Li^7, Ca^{40}, Fe^{56}, Li^6, C^{12}, Pd^{106} and Cd^{113}. Of these Cd is an impurity that was unexpected.

EPMA on the electrode 5 surface and cross section showed no extensive contamination and predominantly Pd. The near surface composition examination by SIMS and Auger is currently underway. EPMA on electrode 17, a 0.5 mm wire, run at extremely high current densities of greater than 3000 mA/cm^2 shows extensive Pt transfer from anode to cathode. Pt concentration on the surface observed range from 30-40% with the remainder being predominantly Pd.

BULK ISOTOPIC ANALYSIS

SIMS analysis of the palladium cathode JM2 and a reference pure palladium sample were analysed using a primary beam of 10.5 keV O_2^+ and positive spectrometry. Small deviations of isotopic abundance compared to pure Pd reference is noted but considered not significant.

ROOM TEMPERATURE MASS SPECTROMETRY

H, H_2, HD and D_2 were found but no evidence of He^4 was found.

SCANNING ELECTRON MICROSCOPY

Scanning electron microscopy on the electrode JM2 showed half the surface covered with pits. Whether it was present prior to testing is not known. Pits were covered with a

thin oxide layer. Evidence of S and Ca on the surface were found. Grain boundaries were deeply etched but no apparent composition difference across the boundary was observed. Electrode 5 as mentioned earlier, showed extensive micro and macro cracks.

DIFFERENTIAL SCANNING CALORIMETRY OF DEUTERATED CATHODES

DSC was done on small pieces of electrode 5 and electrode 17 in an argon atmosphere at a scannning rate of 10°/minute. Figures 6 show the DSC data for electrode 5. The initial endothermic peak corresponds to D desorption. The amount of D desorbed is small indicating that in this extensively cracked electrode the bulk of the deuterium had already desorbed prior to the DSC run. The exothermic peaks around 350°C from points 2-4 correspond to recovery and recrystallization processes.

DETERMINATION OF D/Pd RATIO

Monitoring the D/Pd ratio may be done by measuring the resistivity change, dilation, shift in rest potential, or gravimetry. All methods have certain drawbacks, making estimation of D/Pd ratio difficult. Most of these measurements are most likely to overestimate the measured D/Pd ratio when there is cracking or deformation and any data presented must be used with caution. While gravimetry is direct, in-situ measurement is difficult due to bubble evolution, and density change due to internal cracks. Defects introduced during charging can influence resistivity values. Cracks or fissures and plastic deformation can influence D/Pd estimation. In-situ dilatometry was adopted in this work for the D/Pd ratio estimation because of the relative ease of the technique. Use of intermittent diameter measurements and gravimetry to correlate dilation to D/Pd ratio allows reasonable prediction of D/Pd ratio. Errors due to internal and external cracks and bending of the rods can introduce errors. However, this technique allows one to evaluate effects of different variables such as poisons, current density, surface treatments and microstructure on the D uptake of the electrode with relative ease. Figure 7 shows the length change as a function of charging time of 99.995 Pd cathode with no surface treatments at a current density of 100 mA/cm^2 in a 0.1 molar LiOD. In about 4-5 days, a plateau in the loading versus time curve was reached. Weight and diametral measurements of the electrode were done immediately after the electrolysis was stopped and were used in conjunction with the axial dilation value to determine the D/Pd loading. Loading beyond a D/Pd ratio of 0.93 has been observed using 100 mA/cm^2 current density in LiOD. Higher loadings may be possible with increase in current density, lower temperatures, change electrolyte pH or with the addition of poisons. Figure 7 shows change in dilation in an annealed Pd rod initially at a current density of 100 mA/cm^2, then increased to 200 mA/cm^2, then with the addition of arsenic poison in the form of arsenate to the electrolyte, the power switch off and finally anodic discharge. The original length is not regained after the entire cycle. Change due to increase in current density is small and includes the small length change due to change in cell temperature. Addition of the poison did not have much effect. Turning the power off results in a rapid length change in the first two hours. In another experiment, even after several weeks, we find no change in length until the anodic discharge is done, indicating the metastable nature of the deuteride. These studies are continuing at the present time.

The hydrogen pressures vary exponentially with overvoltage (deviation from the equilibrium voltage at which the forward and reverse rates for this reaction are equal) and astronomical pressures can exist at the cathode/electrolyte interface. Such high surface pressures and favorable surface conditions can increase the uptake of D or H in the metal. D atoms absorbed into the metal occupy octahedral sites, first forming the random solid solution and at higher pressures forming an ordered β phase. The β phase can reach stoichiometry at high pressures such as that obtained during electrolysis at high overvoltages. In this PdD_x interstitial metallic alloy, deuterium has a metallic behavior. This hydride phase has metallic character and D in PdD is considered a deuteron. No clear picture of the behavior of the stoichiometry phase exists at this time. The hydrogen /deuterium loading level in Pons-Fleischmann type cells is much larger than that normally encountered in electroplating, hydrogen storage or conventional metals processing situations. Even in those conventional levels of H or D in metals, understanding of the behavior of H or D is still far from complete.

NUCLEAR RADIATON MONITORING

The nuclear monitoring capabilities of the Physics group at NCFI include (a) A 4" × 8" diameter sodium iodide crystal with associated electronics giving the capability of sensitive measurements of all gamma rays with energies in the range 0.5 MeV to 25 MeV, (b) A HP Ge detector with associated power supplies, amplifiers and multichannel analyzer, giving the capability of giving high resolution measurement of gamma rays in the range from 5 keV to 10 MeV. This system complements the sodium iodide detector, having a lower efficiency and a higher resolution, (c) A Si(Li) detector with the capability of measuring x-rays with energies between 1 keV and 60 keV and (d) A neutron spectrometer with large-area cosmic-ray veto counters to make low-level neutron study possible. Beckman scintillation unit capable of automatic measurement of several hundred samples per day is used for routine tritium monitoring of the cells.

REPRODUCIBITY AND FUTURE OF COLD FUSION RESEARCH

Table 1 lists the different variables that we currently feel are involved in these experiments. Questions about the electrode material, probable involvement of a third element in the nuclear process, contaminants from the electrolyte or cell wall that may influence the surface reaction are currently being asked and are being examined.

Palladium rods during routine casting and drawing are likely to pick up carbon from the molds of the extrusion die. Also trace amounts of O, N, and H are likely to be picked up during fabrication and handling. The levels of these interstitial impurities is likely to be different in electrodes used by different investigators. All these interstitials will compete for the octahedral sites and will reduce the maximum Pd/D ratio. Also these elements may likely block potential defect sites that may be involved as they normally segregate to these defect sites. Unique atomic configurations are possible at special grain boundaries which may likely assist the D-D fusion in the palladium lattice.

Other critical variables include critical loading ratios of deuterium/Pd, surface chemistry of the palladium electrode, the electrolyte composition, temperature, role of lithium, role of deuterium recombination poisons, and rapid variations in operating conditions such as current density required to initiate the heat bursts.

This large number of variables require statistically large numbers of experiments to isolate the conditions under which fusion at room temperature may occur. The fact that a significant but a small number of well established research groups have been able to reproduce some aspects of this effect, requires that research in cold fusion continue on a larger accelerated scale. Currently work is in progress to systematically examine some of the key metallurgical and electrochemical variables.

ACKNOWLEDGEMENTS

Many graduate students and faculty have contibuted to this work in particular Prof. J.G. Byrne, Prof. Rajamani, Dr. John Peterson, Jun Li, Ilesh Shah, H. Hwang, Narendran Karattup, Jose Hevia and Jim Noland and their contribution is gratefully acknowledged. We are thankful to Dr. John Morrey of Battelle Northwest Laboratories, for the help with surface analytical work. We are also thankful to the Physics group at NCFI for their help with nuclear radiation monitoring.

REFERENCES

[1] M. Fleischmann, S. Pons, and M. Hawkins, J. Electroanal. Chem., 261 (1989) 301.
[2] R.C. Kainthla, O. Velev, N.J.C. Packham, L. Kaba, and J. 'O.M. Bockris, Proc. of NSF/EPRI conf. on Cold Fusion, Washington, D.C., October, 1989.
[3] S. Srinivasan and A.J. Appleby, Proc. of NSF/EPRI conference on Cold Fusion, Washington, D.C., October, 1989.
[4] M. McKubre, Proc. of NSF/EPRI Conf. on Cold Fusion, Washington, D.C., October 1989.
[5] A. Azdic, D. Gervasio, I. Bae, B. Cahan and E. Yeager, Personal Communication, Feb., 1990.
[6] P.K. Iyengar, Fifth Intl. Conf. on Emerging nuclear Systems, Karlsruhe, FRG, July, 1989.
[7] Government of India, Atomic Energy Commision Report BARC-1500, P.K. Iyengar and M. Srinivasan, Eds., Dec, 1989.
[8] A. Belzner, U. Bischler, S. Crouch-Baker, T. Gur, G. Lucier, M. Schreiber and R. Huggins, Proc. of Workshop on Cold Fusion Phenomenon, Santa Fe, New Mexico, May 1989.
[9] C.D. Scott, J.E. Mrochek,
E. Newman, T.C. Scott, G.E. Michaels and M. Petek, DOE Report ORNL/TM-11322, November, 1989.
[10] D. Hutchinson, Personal Communication, Feb., 1990.
[11] R.A. Oriani, J.C. Nelson, S.K. Lee and J.H. Broadhurst, Submitted to Nature (1989).
[12] K. Wolf, D.E. Lawson, J.C. Wass and N.J.C. Packham, Proc. of the NSF/EPRI Conf. on Cold Fusion, Washington, D.C., October, 1989.
[13] E. Storms and C. Talcott, J. Fusion Tech., in Press (1990).
[14] R. Taniguchi, T. Yamamoto, and S. Irie, Jap. J. Appl. Phy., 28 (1989) 2021.

Table 1. Some of the known variables involved in electrolytic cold fusion experiments.

1. EXPERIMENTAL CONDITIONS
    - CURRENT DENSITY
    - TEMPERATURE
    - ELECTROLYTE COMPOSITION
    - POISONS IN ELECTROLYTE
    - NEED FOR INITIATION (ELECTRICAL, MAGNETIC, THERMAL or ULTRASONIC SHOCK)
    - H, CO_2 PICK UP
    - CELL DESIGN

2. ELECTRODE PURITY
    - SUBSTITUTIONAL IMPURITIES
        - PRIMARY Pd (Cu, Ni, Fe, Zr, Te, As, Sb, Cd, Mg, Ca, Li...)
        - RECYCLED Pd (LARGE NO. OF ALLOYING ELEMENTS)
    - INTERSTITIAL IMPURITIES
        - PICKED UP DURING PROCESSING & HANDLING (C, O, N, H)

3. IMPURITIES IN ELECTROLYTE
    - IMPURITIES FROM PROCESSING & HANDLING (C, S, Cu, Zr...)

4. ELECTRODE MICROSTRUCTURE
    - GRAIN SIZE, DISLOCATION DENSITY & DISTRIBUTION

5. POSSIBLE ROLE OF A THIRD ELEMENT IN THE NUCLEAR REACTION

6. CELL DESIGN: ELECTRODE GEOMETRY, ELECTRODE SPACING, ETC.

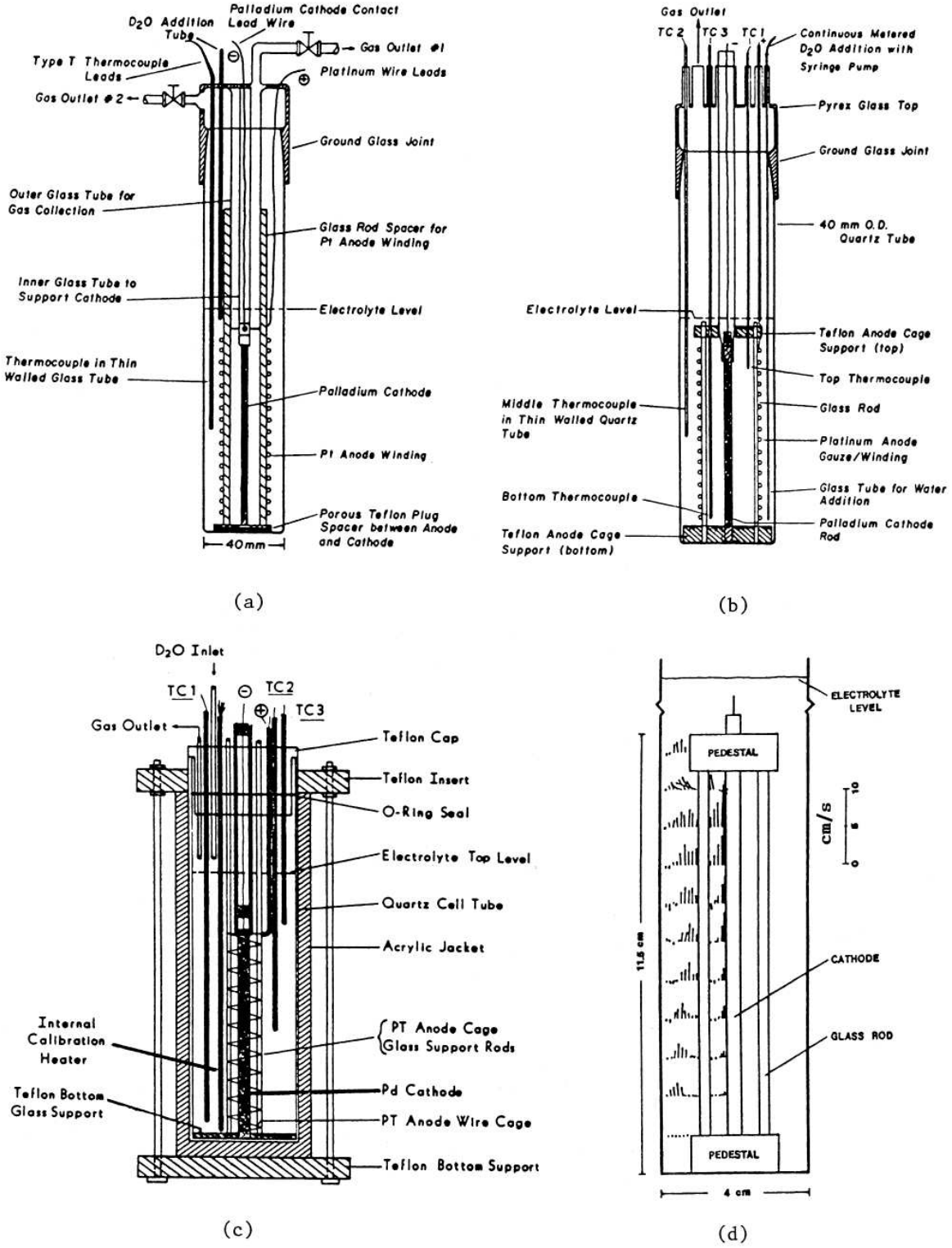

Figure 1. (a, b & c) Different electrolytic cell configurations used and (d) Laser Doppler measurement of gas bubble velocities in the electrolyte under typical operating conditions of cell 1a.

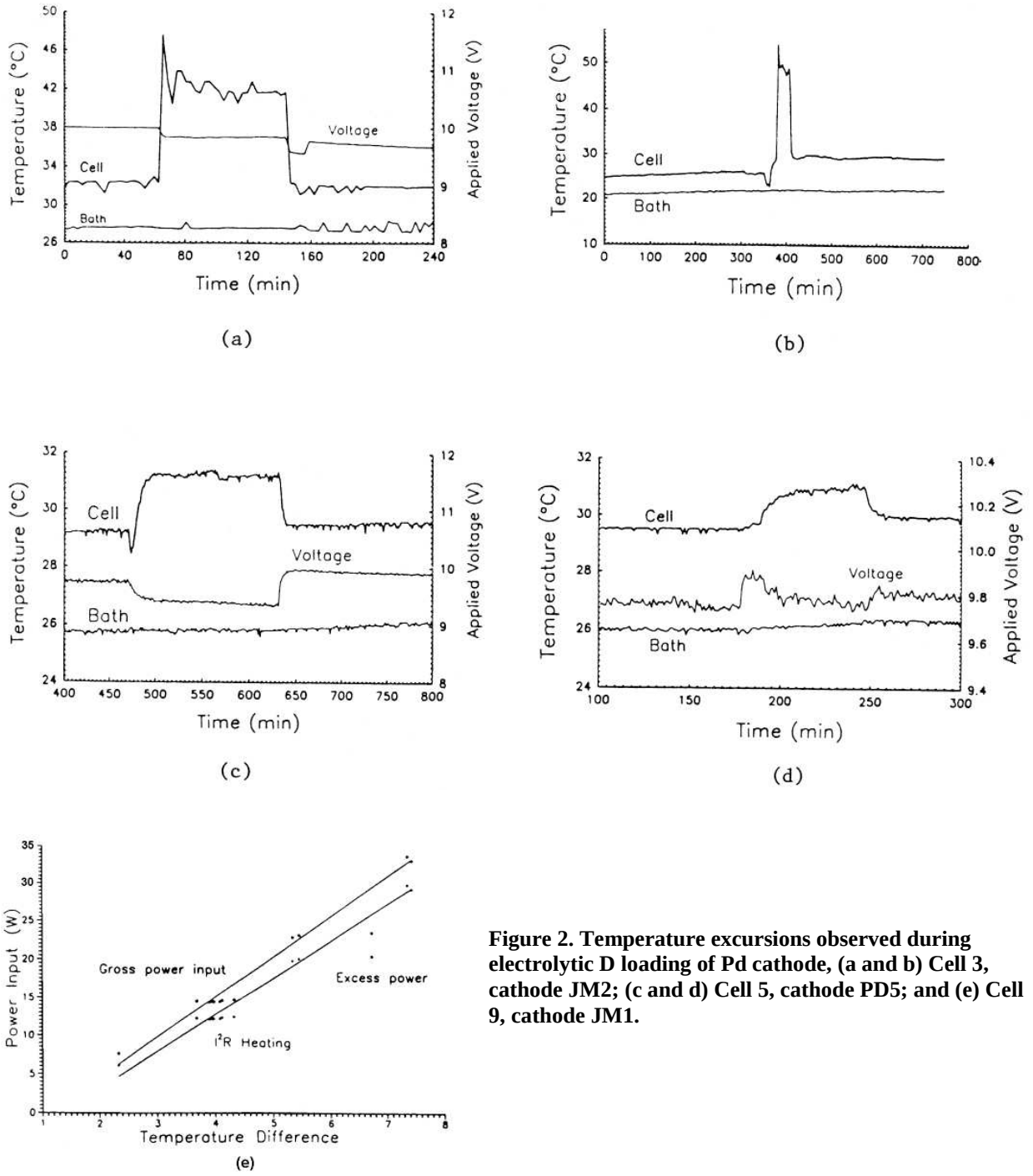

Figure 2. Temperature excursions observed during electrolytic D loading of Pd cathode, (a and b) Cell 3, cathode JM2; (c and d) Cell 5, cathode PD5; and (e) Cell 9, cathode JM1.

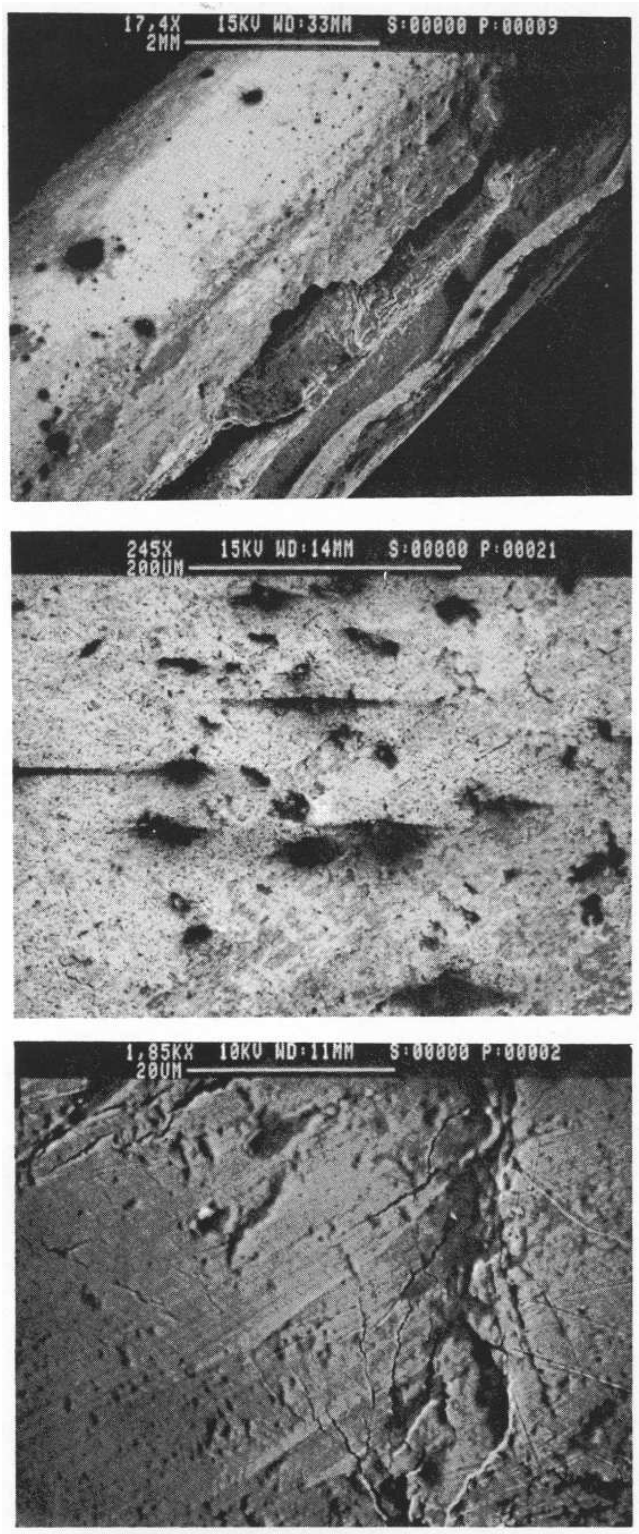

(a)

(b)

(c)

Figure 3. Scanning electron micrographs showing extensive cracking in palladium cathode 5 after 11 months of D charging, (a and b) Surface region; and (c) interior region of the cathode.

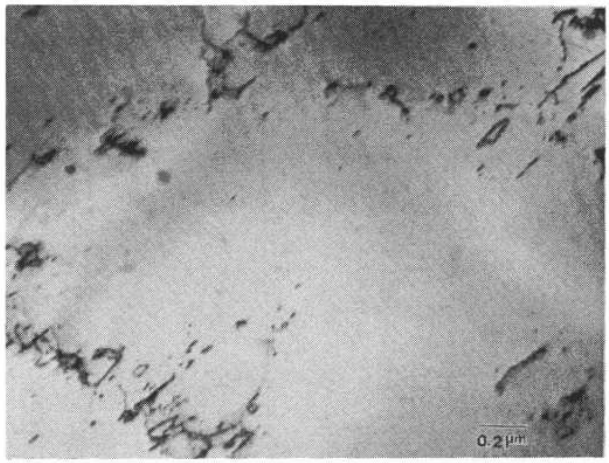

(a)

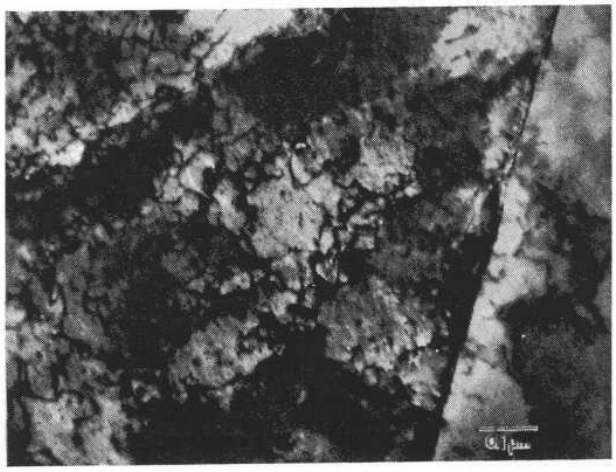

(b)

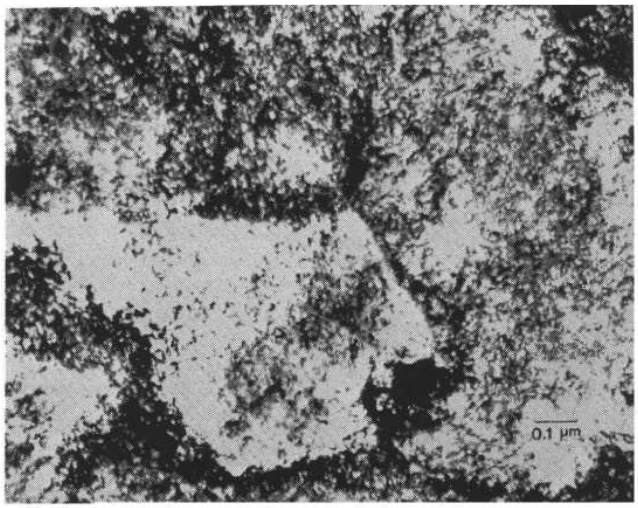

(c)

Figure 4. TEM micrographs of palladium cathodes. (a) After annealing at 600°C for 1 hour (Electrode JM2); (b) after deuterium loading for 3 weeks (Electrode JM2); and (c) after 11 months of deuterium loading (Electrode 5).

Table 2. AES analysis of the near surface region of Pd cathode JM2 after the heat burst shown in figure 2a.

ELEMENT	SIGNAL	SENS. FACTOR	AT%
Si	0.45	0.25	5.71
S	0.40	0.75	1.83
Cl	0.59	1.00	2.02
C	2.14	0.14	52.37
Pd	1.00	0.85	4.01
O	2.48	0.40	21.24
Cu	0.34	0.23	< 5.07
Na	0.38	0.25	5.14
Co	0.18	0.23	< 2.61

Table 3. XPS analysis of the near surface region of Pd cathode JM2 after heat burst in figure 2a.

ELEMENT	SIGNAL	SENS. FACTOR	AT%
Si	0.03	0.27	2.31
C	0.78	0.25	64.52
Pd	0.28	2.70	2.16
O	0.89	0.60	30.62
Cu	0.06	4.20	0.30
Sn	0.01	4.30	0.05
Co	< 0.01	0.23	< 0.04

Table 4. Ratio of Li and Pd signals as a function of sputtering time of the surface of Pd cathode JM2 after heat burst shown in figure 2a.

TIME mts	Pg^{106} Cts.	Li^{7} Cts.	Li/Pd
0.00	1876	96159	51.26
10.00	966	28534	29.54
20.00	730	15002	20.55
30.00	674	10331	15.33
40.00	596	8171	13.71
50.00	567	6675	11.77
60.00	486	5855	12.05
70.00	450	5328	11.84
80.00	446	4885	10.95
90.00	442	4407	9.97

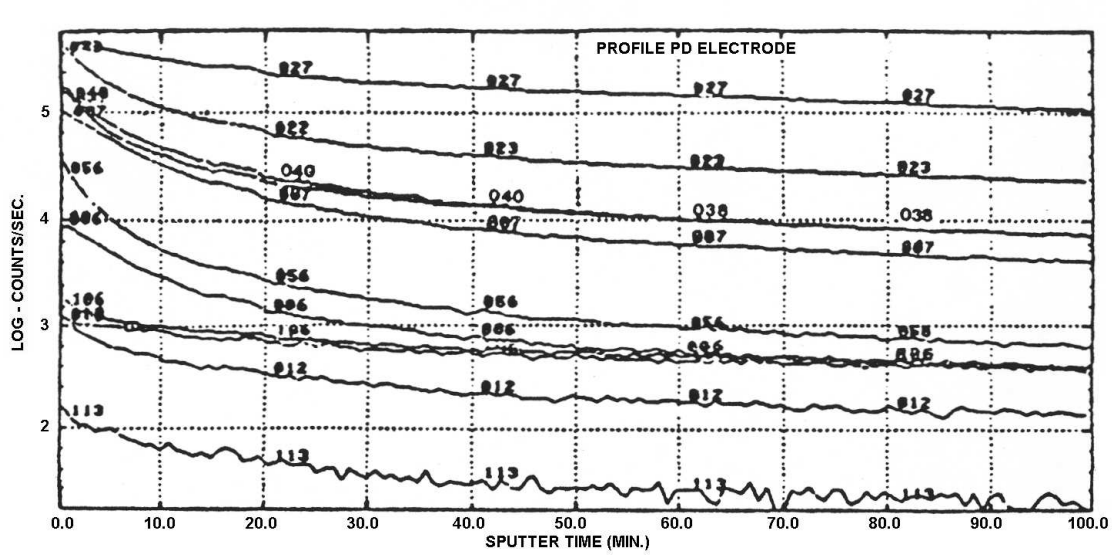

Figure 5. SIMS profile of palladium cathode JM2 after heat burst shown in figure 2a.

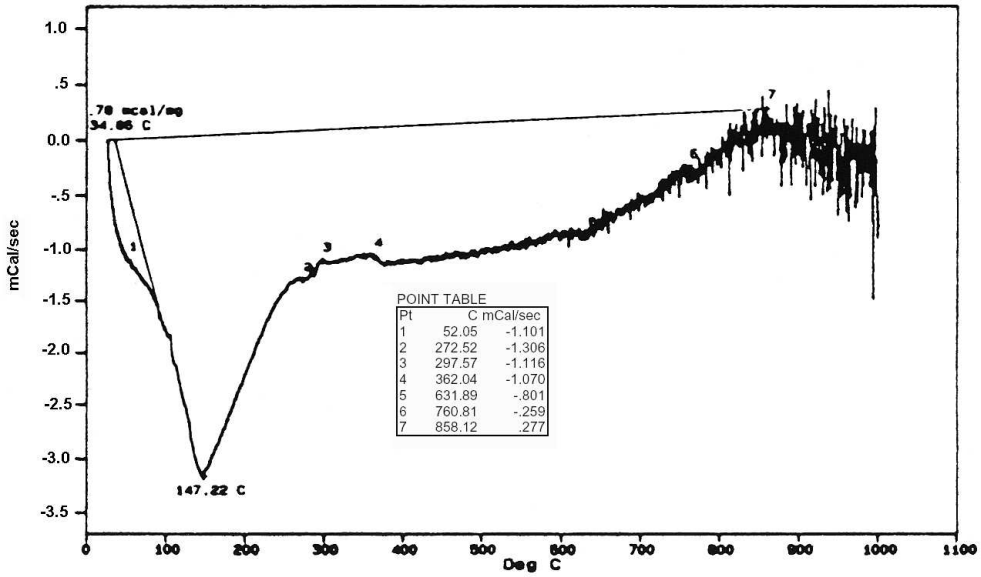

Figure 6. DSC scan of Pd cathode 5 after 11 months of electrolytic charging and three temperature excursion events.

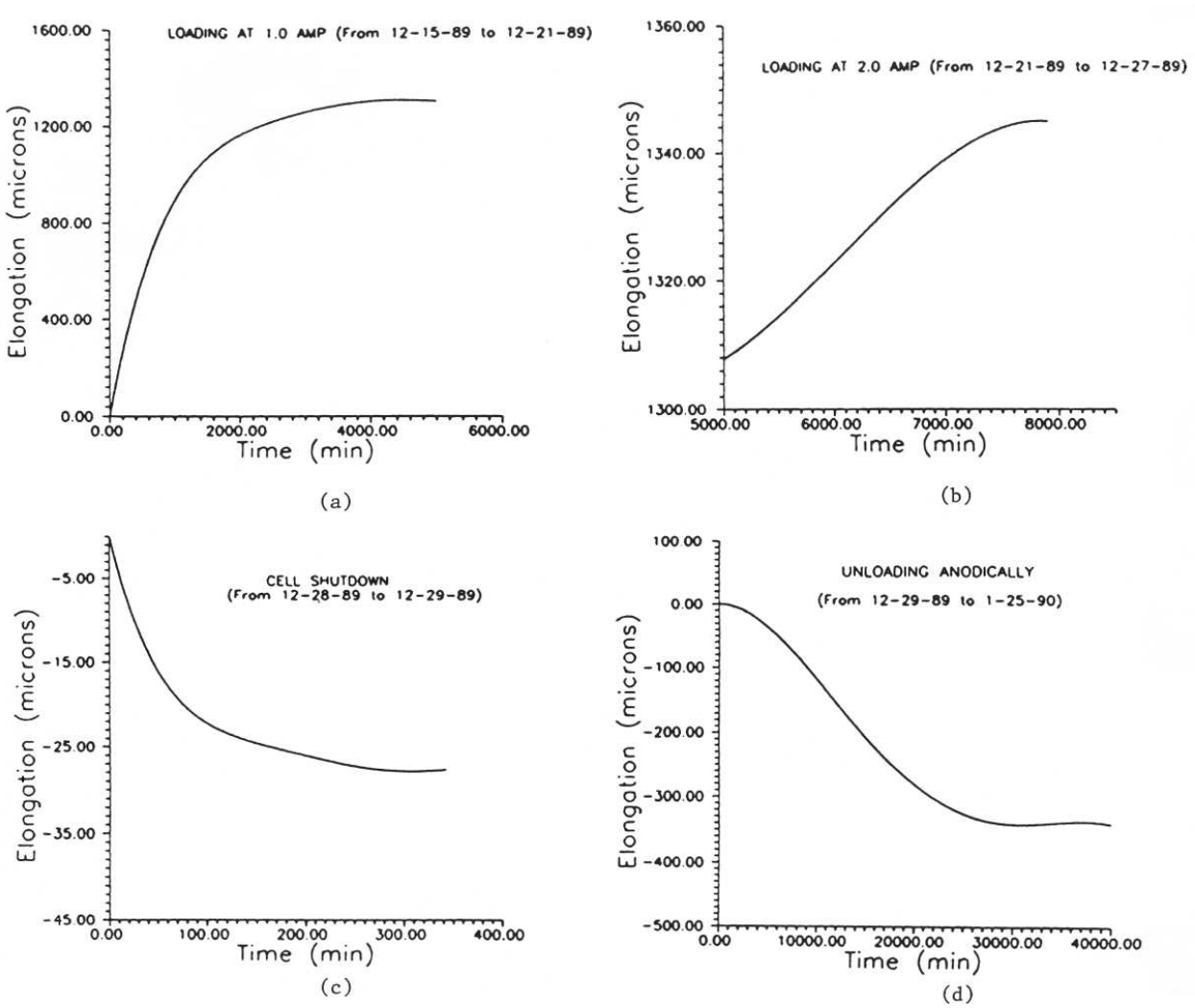

Figure 7. Electrode elongation measured in-situ during (a) loading at 100 mA/cm^2, (b) after current density change to 200 mA/cm^2, (c) after power was turned off and (d) during anodic D discharge.